

---

# Aurora Borealis: Stochastic Cellular Automata Simulations of the Excited-State Dynamics of Oxygen Atoms

---

PAUL G. SEYBOLD,<sup>1</sup> LEMONT B. KIER,<sup>2</sup> CHAO-KUN CHENG<sup>3</sup>

<sup>1</sup>Departments of Chemistry and Biochemistry, Wright State University, Dayton, Ohio 45435

<sup>2</sup>Department of Medicinal Chemistry, Virginia Commonwealth University, Richmond, Virginia 23298

<sup>3</sup>Department of Mathematical Sciences, Virginia Commonwealth University, Richmond, Virginia 23298

Received 1 March 1999; revised 3 April 1999; accepted 8 April 1999

---

**ABSTRACT:** Emissions from the  $^1S$  and  $^1D$  excited states of atomic oxygen play a prominent role in creating the dramatic light displays (aurora borealis) seen in the skies over polar regions of the Northern Hemisphere. A probabilistic asynchronous cellular automaton model described previously [Seybold, Kier, and Cheng, *J Phys Chem* 1998, 102, 886–891] has been applied to the excited-state dynamics of atomic oxygen. The model simulates the time-dependent variations in ground ( $^3P$ ) and excited-state populations that occur under user-defined probabilistic transition rules for both pulse and steady-state conditions. Although each trial simulation is itself an independent “experiment,” deterministic values for the excited-state emission lifetimes and quantum yields emerge as limiting cases for large numbers of cells or large numbers of trials. Stochastic variations in the lifetimes and emission yields can be estimated from repeated trials. © 1999 John Wiley & Sons, Inc. *Int J Quant Chem* 75: 751–756, 1999

**Key words:** cellular automata; oxygen; excited states; aurora borealis; northern lights

---

## Introduction

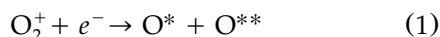
In Roman mythology Aurora was the goddess of the dawn, who rose each morning from the ocean and brought light to Earth. The Greeks called her Eos. The aurora borealis, or northern lights, is

*Correspondence to:* P. G. Seybold.

a dramatic light display that appears occasionally in the upper atmosphere in northern latitudes [1–3]. The corresponding display in the south polar regions is called aurora australis. Similar emissions can be detected from the atmospheres of Mars and Venus.

It is now known that emissions from excited oxygen atoms play a prominent role in these displays. Recent experimental and theoretical work

suggests that an important channel for formation of these excited atoms is dissociative recombination of  $O_2^+$ , formed during the day by ultraviolet irradiation in the ionosphere, with cold electrons [4, 5]:



(Here  $O^*$  and  $O^{**}$  represent potentially excited oxygen atoms.) Other processes also produce excited oxygen atoms, including the photolysis of ozone,  $O_3 + h\nu \rightarrow O^* + O_2$  [6]. Three states arise from the atomic oxygen  $p^4$  configuration [7]; a  $^1S$  state at  $33,792 \text{ cm}^{-1}$  (4.189 eV), a  $^1D$  state at  $15,868 \text{ cm}^{-1}$  (1.967 eV), and the ground  $^3P$  state, with  $J = 0, 1,$  and  $2$  sublevels at 226.5, 158.5, and  $0 \text{ cm}^{-1}$ , respectively. These states are illustrated in Figure 1. The prominent aurora green line at  $5577 \text{ \AA}$  is caused by the forbidden  $^1S \rightarrow ^1D$  transition. Red lines at  $6300 \text{ \AA}$  and  $6364 \text{ \AA}$  come from  $^1D \rightarrow ^3P$  transitions, and an ultraviolet line at  $2972 \text{ \AA}$  arises from the  $^1S \rightarrow ^3P$  transition. All of these transitions are forbidden by the LaPorte rule [8], and the last two are also spin forbidden.

Traditionally excited-state dynamics have been analyzed by solving sets of coupled differential rate equations which describe the interrelationships and transition rates among the states. Although it is not normally made explicit, these equations and their solutions are valid only in the deterministic limits of either (i) very large numbers of particles or (ii) very large numbers of trials

for single particles. We have recently presented an alternative, general model for first-order molecular kinetic processes based on cellular automata [9]. The cellular automata model is stochastic in nature and can be applied to both single ingredients and larger ensembles. Traditional deterministic solutions emerge naturally from the model as limiting cases for either large numbers of ingredients or large numbers of trials. As one application of the model, a general cellular automata treatment of molecular excited-state dynamics has also been introduced [10]. In the present study we present a specific application of the latter excited-state model to the excited-state dynamics of atomic oxygen, as exhibited in the atmospheric displays observed as northern lights.

## Methods

The general concepts of cellular automata have been extensively covered in the literature [11–16], and the features of our own models have also been described [9, 10, 18] so that only a brief summary will be given here. Cellular automata typically treat systems composed of ingredients which occupy the cells of one-, two-, or three-dimensional grids. Normally the ingredients, which in the present case represent oxygen atoms, can move to unoccupied cells and may also be capable of changing their states, these actions being determined by local rules specified by the model. Time steps occur as discrete iterations in which the rules are applied. The ensemble of ingredients evolves in time in accordance with the specified rules and may exhibit quite complex behaviors (characterized as “emergent properties”) even when relatively simple rules are employed.

In the present first-order model a two-dimensional  $N \times M$  (usually  $100 \times 100$ ) rectangular grid is used, movement rules are unnecessary, and only probabilistic state-transition rules are invoked [9, 10]. The latter probabilistic rules govern the likelihood of transitions between the states of the oxygen atoms. During each iteration, all of the ingredients in the grid are interrogated in random order and given an opportunity to act; hence the automata to be described are *asynchronous*. (The order of interrogation is immaterial in the present work but can be important in other studies, e.g., when the transition probabilities depend on the natures of the neighboring cells.) A visual display

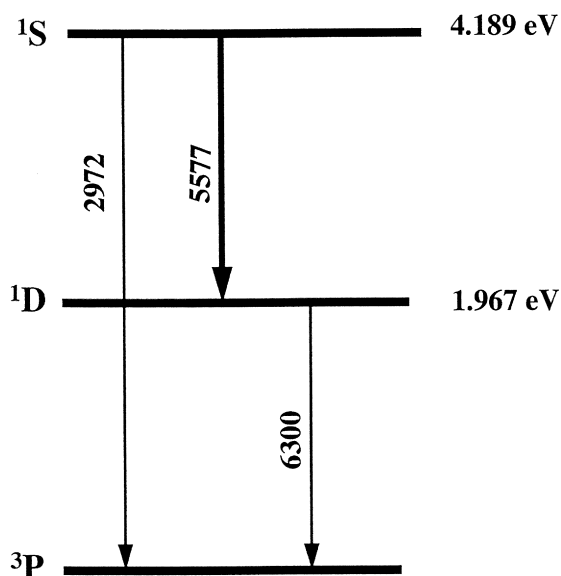


**FIGURE 1.** Excited states and transitions of atomic oxygen.

of the model's evolution is provided in which the oxygen atomic states are represented by different colors of the cells of the grid, and an inventory is kept of the numbers of cells of different colors and their transitions as the system evolves. Because of the probabilistic rules, each trial simulation is an independent "experiment." Statistical information can be obtained by performing repeated trials and analyzing the results.

The transition probabilities between the states were obtained from the compilation of Okabe [18] and are as follows:

$$\text{Prob}({}^1S \rightarrow {}^3P): 0.067 \text{ s}^{-1}$$

$$\text{Prob}({}^1S \rightarrow {}^1D): 1.34 \text{ s}^{-1}$$

$$\text{Prob}({}^1D \rightarrow {}^3P): 0.0051 \text{ s}^{-1}$$

Since the probabilities used in the simulations must necessarily all be less than unity, the above figures were divided by 10, so that in effect each iteration in the model corresponds to an elapsed time of 0.1 s.

Three cases were examined: (1) decay starting with all O atoms in the uppermost  ${}^1S$  state, illustrating both direct decay to the  ${}^3P$  state and cascade via  ${}^1D$ ; (2) decay of a mixed population of states representative of the experimentally observed yields [4] of the dissociative recombination of  $\text{O}_2^+$ ; and (3) a steady-state condition in which transitions from the ground  ${}^3P$  state repopulate the excited  ${}^1S$  and  ${}^1D$  states in the same ratio as used in case 2. In the last case, for purposes of illustration, arbitrary probabilities were tested for the repopulation process, the rate of which varies with atmospheric conditions. These last probabilities represent the overall process consisting first of recombination of the oxygen atoms ( $\text{O} + \text{O} + M \rightarrow \text{O}_2 + M$ ) and then ionization of the resulting molecular oxygen ( $\text{O}_2 + h\nu \rightarrow \text{O}_2^+ + e^-$ ).

## Results and Discussion

### CASE 1: DECAY OF THE ${}^1S$ STATE

For this case all cells were initially placed in the  ${}^1S$  state. To illustrate the stochastic character of the model, two model simulations were carried out, the first using a  $20 \times 20 = 400$  cell grid and the second using a  $100 \times 100 = 10,000$  cell grid. The results for the 400-cell simulation are shown in Figure 2. From Figure 2(a) it is apparent that the  ${}^1S$  state quickly decays, essentially disappearing by

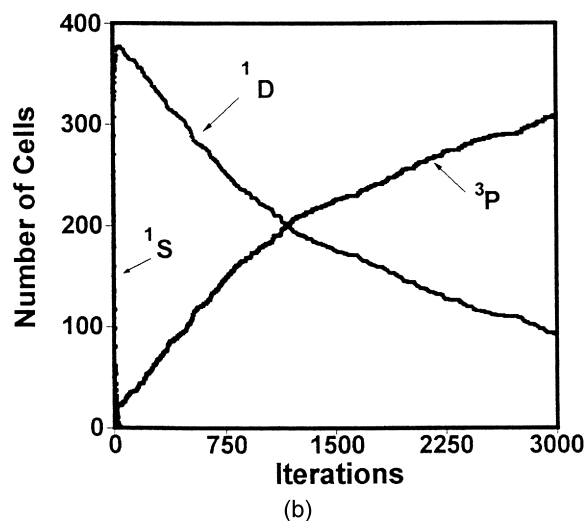
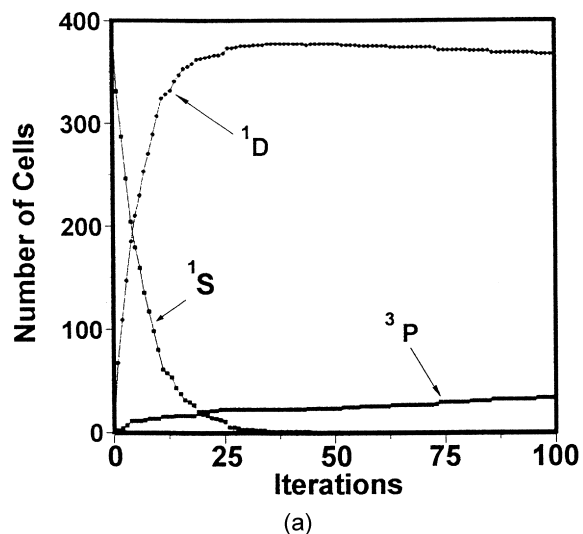


**FIGURE 2.** Variations in the state populations during decay of the  ${}^1S$  state at (a) short times and (b) longer times, as simulated by a 400-cell cellular automaton.

about 30 iterations, corresponding to 3 s elapsed time. The decay path is predominantly to the  ${}^1D$  state, with only a handful of the cells converting to the  ${}^3P$  ground state. As transitions from the  ${}^1S$  state occur the  ${}^1D$  state population increases, reaching a maximum at ca. 25–30 iterations. Thereafter the  ${}^1D$  population begins a slow descent as transitions to the ground state exert their influence. A view of part of the later stages is given in Figure 2(b). Because the number of ingredients involved in the simulation is finite and modest, the population curves are not entirely smooth. (A smaller cell count would display even greater raggedness.)

For a set of 10 trial simulations the half-lives  $\tau_{1/2}$  for decay of the  $^1S$  state ranged from 3.9 to 4.8 iterations, with an average  $\tau_{1/2}(^1S) = 4.5 \pm 0.3$  iterations. Since the lifetime is related to the half-life as  $\tau = \tau_{1/2}/\ln 2$ , this translates to  $\tau_{1/2}(^1S) = 6.5 \pm 0.4$  iterations, or  $0.65 \pm 0.04$  s. The reported value for this lifetime is 0.71 s [12]. The quantum yields  $\phi(^1S \rightarrow ^3P)$  in these same ten trials ranged from 0.0275 to 0.055, showing the highly stochastic nature of the variations found when small numbers of ingredients are involved. The average quantum yield for this transition was  $\phi(^1S \rightarrow ^3P) = 0.043 \pm 0.010$  and that for transition to the  $^1D$  state was  $\phi(^1S \rightarrow ^1D) = 0.957 \pm 0.010$ . The deterministic quantum yields expected on the basis of the transition probabilities are  $\phi(^1S \rightarrow ^3P) = 0.048$  and  $\phi(^1S \rightarrow ^1D) = 0.952$ .

In this same series of trials the  $^1D$  half-life ranged from 1307 to 1481 iterations, with an average  $\tau_{1/2}(^1D) = 1368 \pm 62$  iterations, which corresponds to a lifetime  $\tau(^1D) = 197.4 \pm 0.9$  s. The experimental value given by Okabe is  $\tau = 150$  s [18]. The difference in the lifetime values noted here prompts several comments. First, it is likely that this difference falls well within the normal uncertainty, experimental and theoretical, for such a transition. Lifetimes of long-lived atomic and molecular states are notoriously difficult to measure accurately, since the excited species involved are extremely vulnerable to collisional and other (see below) quenching processes, and the experimental value is given only to two significant figures. It is also clear that the transition probabilities employed are approximate and could easily be adjusted to exactly match the observed lifetime. However, given the uncertainty in the observed lifetime, the latter procedure seems hardly justified in this instance. Since only a single decay channel for the  $^1D$  state is included in the model, the quantum yield of emission for this state is the same,  $\phi = 0.957$ , as its yield via the radiative  $^1S \rightarrow ^1D$  transition.

In contrast to the 400-cell simulation, the simulation with 10,000 cells, a number which approximates the deterministic limit, shows a much smoother variation in the state populations (Fig. 3). Figure 3(a) shows the early stages of this evolution with the rapid decay of the  $^1S$  state and initial buildup of the  $^1D$  state. Figure 3(b) illustrates the later progression toward complete decay to the  $^3P$  state. In Figure 4 the logarithmic decay curves of the  $^1S$  and  $^1D$  states are shown. Both decays are

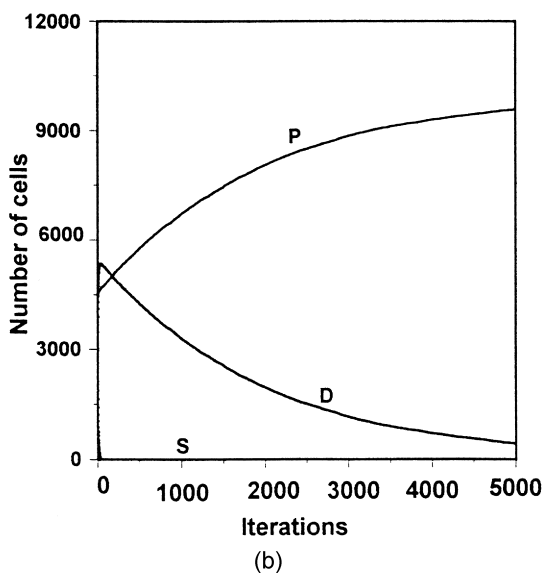
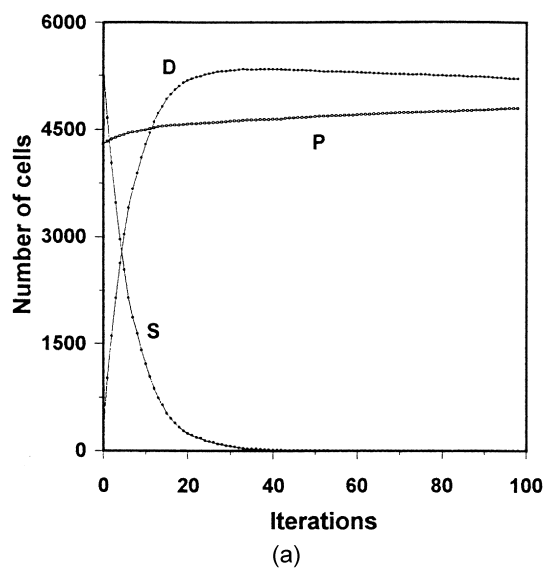


**FIGURE 3.** Variations in the state populations resulting from decay of the  $^1S$  state at (a) short times and (b) longer times as simulated by a 10,000-cell cellular automaton.

seen to approximate the expected exponential falloffs until the numbers of respective ingredients remaining become too small for statistical validity. The lifetime values obtained from fitting the exponential decays for this single trial with 10,000 cells were (ignoring significant figures for purposes of illustration)  $\tau(^1S) = 0.669 \pm 0.004$  s ( $r^2 = 0.998$ ) and  $\tau(^1D) = 199.20 \pm 0.01$  ( $r^2 = 0.9998$  for the interval 70–4500 iterations). The quantum yields for this single run were  $\phi(^1S \rightarrow ^3P) = 0.049$  and

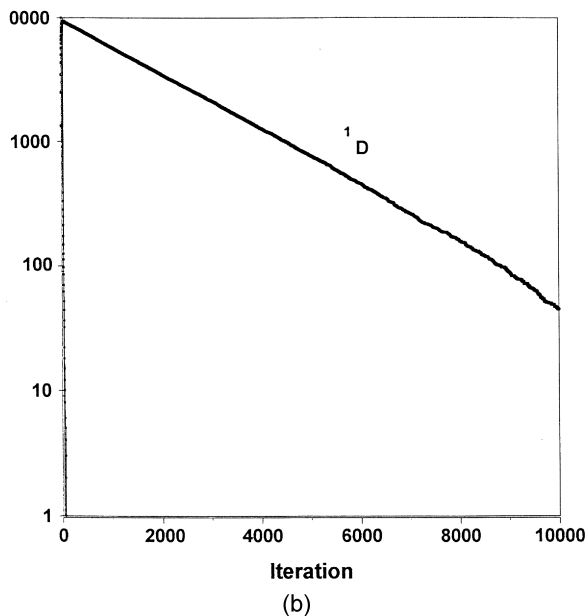
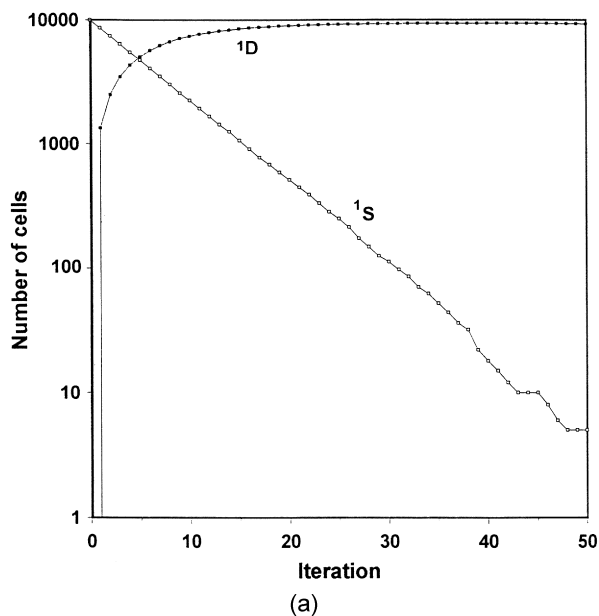


**FIGURE 4.** Decay profiles for (a) the  $^1S$  state and (b) the  $^1D$  state as simulated by a 10,000-cell cellular automaton.

$\phi(^1S \rightarrow ^1D) = 0.951$ , compared to the theoretical yields of 0.048 and 0.952, respectively.

### CASE 2: DECAY OF A DISTRIBUTED POPULATION

Kella et al. [4] have estimated the relative yields of the O atoms produced in the dissociative recombination of  $O_2^+$  [reaction (1)] to be 43% for the  $^3P$

state, 54.5% for the  $^1D$  state, and 2.5% for the  $^1S$  state. A simulation was carried out with the 10,000-cell grid to illustrate the time-dependent population variations arising from such an initial distribution. The results are shown in Figure 5. As in case 1, the  $^1S$  population rapidly disappears, whereas the  $^1D$  population quickly peaks and then more slowly decays while it replenishes the ground  $^3P$  state population.

### CASE 3: STEADY STATE

In this study probabilities for production of both the  $^1S$  and  $^1D$  states from the  $^3P$  state were introduced. The rates were chosen to be consistent with the experimental yields described above for the production of excited oxygen atoms by dissociative recombination [4]. In a first study the transition probabilities were set at  $P_T(^3P \rightarrow ^1S) = 0.000025$  and  $P_T(^3P \rightarrow ^1D) = 0.000545$ . The results for these rates are shown in Figure 6, where it is clear that a high steady-state population of the  $^1D$  state arises because of the long lifetime of this metastable species. A second study (not illustrated) with higher rates for these processes showed an even greater steady-state accumulation in the  $^1D$  state, as well as considerable depletion of the  $^3P$  state. It seems possible that a similar population inversion might occur in the atmosphere in

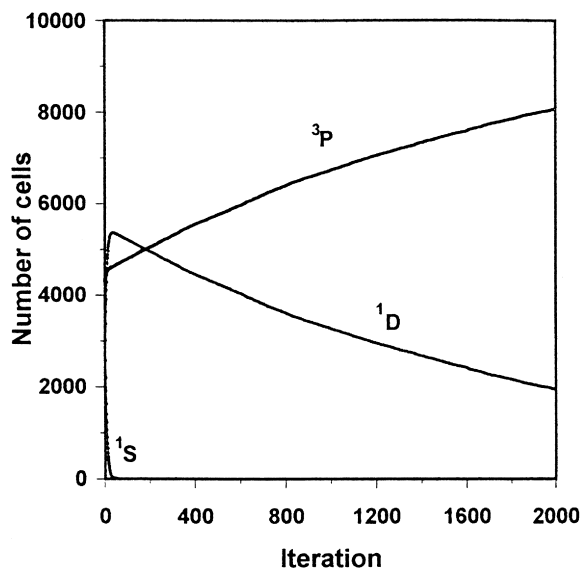


**FIGURE 5.** Time-dependent variations in the state populations following generation of a population representative of dissociative recombination, as simulated by a 10,000-cell cellular automation.

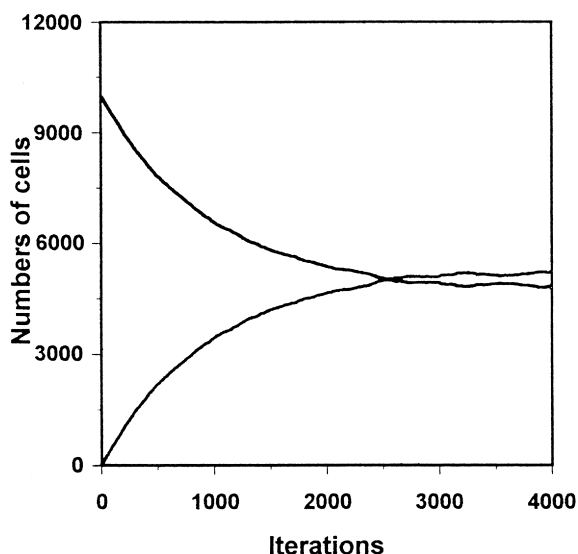


**FIGURE 6.** Approach to steady-state conditions from a population originally in the ground  $^3P$  state.

polar regions when atmospheric conditions are favorable, and it has not escaped our attention that the conditions illustrated in Figure 1, combined with the metastable nature of the  $^1D$  state, are strikingly similar to the classic structure found in a three-state laser. While general atmospheric conditions would hardly seem suitable for laser action *per se*, it does appear possible that stimulated emission might contribute to some (unknown) extent to the decay of the  $^1D$  state in the upper atmosphere, thereby shortening its observed lifetime.

## Conclusions

Three models have been applied to the excited-state dynamics of atomic oxygen to illustrate the ability of relatively simple cellular automata models to simulate the time-dependent variations in the populations of excited- and ground-state atoms in a real experimental milieu. The models, based on reported transition probabilities, provide a consistent picture of the excited-state dynamics of oxygen atoms in the upper atmosphere, including values for the state lifetimes and quantum yields of emission. An interesting outgrowth of the steady-state model is the conjecture that stimulated emission may contribute to the decay of the

long-lived  $^1D$  state. Cellular automata models can supplement or even, in some applications, replace the traditional approach to such problems, which relies on the solution of a set of coupled differential equations. Since the cellular automata models are based on a simple set of rules and operate on finite elements, we argue that such models have an attractive heuristic quality and correspond more closely to the experimental situation on the atomic and molecular level than do the abstract equations. In addition, the cellular automata models provide stochastic and statistical information that is missing from the traditional approach.

## References

- Petrie, W. *KEOEIT: The Story of the Aurora Borealis*; Pergamon: New York, 1963.
- McCormac, B. M. *Aurora and Airglow*; Reinhold: New York, 1967.
- Davis, N. *The Aurora Watcher's Handbook*; University of Alaska Press: Fairbanks, 1992.
- Kella, D.; Vejby-Christiansen, L.; Johnson, P. J.; Pederson, H. B.; Andersen, L. H. *Science* 1997, 276, 1530–1533.
- Guberman, S. L. *Science* 1997, 278, 1276–1278.
- Ravishankara, A. R.; Handcock, G.; Kawasaki, M.; Matsumi, Y. *Science* 1998, 280, 60–61.
- Winn, J. S. *Physical Chemistry*; Harper Collins: New York, 1995.
- Noggle, J. H. *Physical Chemistry*, 3rd ed.; Harper Collins: New York, 1996, p. 738.
- Seybold, P. G.; Kier, L. B.; Cheng, C.-K. *J Chem Info Comput Sci* 1997, 37, 386–391.
- Seybold, P. G.; Kier, L. B.; Cheng, C.-K. *J Phys Chem* 1998, 102, 886–891.
- Burks, A. W. *Essays on Cellular Automata*; University of Illinois Press: Urbana, 1970.
- Schroeder, M. *Fractals, Chaos, Power Laws*; Freeman: New York, 1991, Chap. 17, p. 371.
- Farmer, D.; Toffoli, T.; Wolfram, S. Eds., *Cellular Automata*; North-Holland: New York, 1984.
- Toffoli, T.; Margolus, N. *Cellular Automata Machines: A New Environment for Modeling*; MIT Press: Cambridge, MA, 1987.
- Wolfram, S. *Cellular Automata and Complexity*; Perseus Press: New York, 1994.
- Chopard, B.; Droz, M.; Chopard, B. *Cellular Automata Modeling of Physical Systems*; Cambridge University Press: New York, 1998.
- Kier, L. B.; Cheng, C.-K.; Testa, B. *Future Generations Comput Systems*, to appear.
- Okabe, H. *Photochemistry of Small Molecules*; Wiley: New York, 1978, p. 370.